A Speed Regulator for A Torque–Driven Inertia Wheel Pendulum by Bounded Torque [1]

Jesús Sandoval *, **Rafael Kelly** **, **Víctor Santibánez** ***

* *Tecnológico Nacional de México, Instituto Tecnológico de La Paz, Blvd. Forjadores de B.C.S., La Paz, B.C.S., 23080, MÉXICO* *e–mail:* jesus.sg@lapaz.tecnm.mx,
** *División de Física Aplicada, CICESE, Ensenada, B.C., 22800 MÉXICO, e–mail:* rkelly@cicese.edu.mx,
*** *Tecnológico Nacional de México, Instituto Tecnológico de La Laguna, Apdo. Postal 49, Adm. 1, Torreón, Coahuila, 27001, MÉXICO* *e–mail:* vsantiba@itlalaguna.edu.mx

Abstract: A speed regulator for the inertia wheel pendulum has been reported recently in the literature based on an alternative energy shaping and damping injection approach. This controller achieves that the wheel rotates at a small constant speed and it drives the pendulum to its upward position. In the present paper, we are interested in enhancing the control system for small desired constant wheel speed by the practical capability of maintaining the computed torque input inside prescribed limits. The perfomance of the proposed controller is illustrated via simulations, which have been compared with those reported in the literature.

Keywords: Underactuated mechanical system, bounded control, Lyapunov theory.

1. INTRODUCTION

Nowadays, there are few researches addressing the speed regulation of underactuated mechanical systems (see e.g. Sandoval et al. (2020); Romero et al. (2016); Delgado & Kotyczka (2016)). The speed regulation for underactuated mechanical systems has been formulated mainly in the following way: to design a controller capable of asymptotically driving the nonactuated joints to a proper constant position, and the actuated joints to rotate at a suitable desired constant speed. Some approaches that have successfully solved this problem are: a PID controller introduced by Romero et al. (2016); an energy shaping controller for a wheeled inverted pendulum reported by Delgado & Kotyczka (2016) based on the Controlled Lagrangian method (see Bloch et al. (2000)); and recently, an energy shaping and damping injecton approach has been introduced to design a speed regulator for a torque–driven inertia wheel pendulum presented by Sandoval et al. (2020). This latter approach is inspired in the IDA-PBC method published by Ortega et al. (2002).

The purpose of the present research is to improve the performance of the controller reported in Sandoval et al. (2020), when dealing with prescribed bounded torque input as an additional criterion of the designed controller. To this end, we follow the strategy given by Santibáñez et al. (2005) in the position regulation problem, but now applied to speed regulation control, so that, we have introduced a slight change in the designed controller by Sandoval et al. (2020), and we have carried out a proper tuning of its gains to ensure that the actuator allowed torque remains inside prescribed limits.

The inertia wheel pendulum is an underactuated mechanical system consisting of a physical frictionless pendulum with a symmetric actuated (via an ideal torque actuator) disk (wheel) attached to the pendulum distal tip, which is free to spin about an axis parallel to the axis of rotation of the pendulum (see Figure 1). Underactuated nature is because it has two degrees–of–freedom and only one actuator located at the disk, which is assumed to be an ideal (memoryless linear identity) torque device.

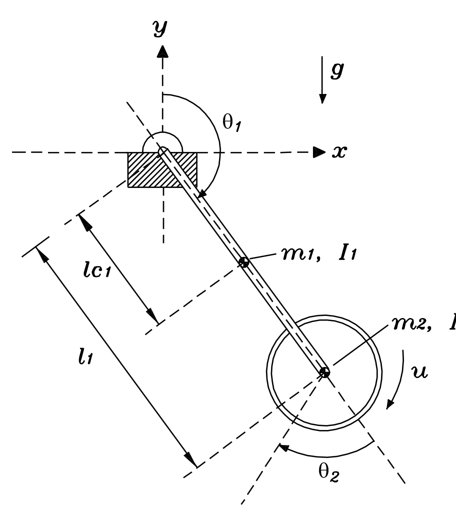

Fig. 1. Sketch of a torque–driven inertia wheel pendulum.

[1] This work was partially supported by CONACyT grants 166636, 166654 and 134534, and by TecNM Projects.

Throughout this paper, we use the notation $(\cdot)_{2\times 2}$ to indicate a 2×2 matrix, with $I_{2\times 2}$ as the identity matrix and $0_{2\times 2}$ the matrix of zeros; while $\mathbf{0}_2 \in \mathbb{R}^n$ is the 2×1 vector of zeros, $\nabla_{(\cdot)} = \frac{\partial}{\partial(\cdot)}$, and $\det[A]$ denotes the determinant of the square matrix A.

This paper is organized as follows. Section 2 summarizes the inertia wheel pendulum model and control problem formulation. In Sections 3 and 4, we introduce the proposed controller and our stability analysis, respectively. Simulations results on an inertia wheel pendulum are given in Section 5. Finally, we offer some concluding remarks in Section 6.

2. CONTROL PROBLEM FORMULATION

The formulation begins with a Hamiltonian–like mathematical description of the torque–driven inertia wheel pendulum, where the energy function (Hamiltonian) is the sum of the kinetic energy plus energy potential of the mechanical system

$$H(\boldsymbol{q}, \boldsymbol{p}) = \frac{1}{2}[a_1 p_1^2 + 2a_2 p_1 p_2 + a_3 p_2^2] + m_3[\cos(q_1) - 1], \tag{1}$$

where $\boldsymbol{q} = [q_1 \;\; q_2]^T = [\theta_1 \;\; \theta_2]^T$ and $\boldsymbol{p} = [p_1 \;\; p_2]^T$ are the vectors of generalized positions and momenta, respectively, the M inertia matrix is given by

$$M = \begin{bmatrix} a_1 & a_2 \\ a_2 & a_3 \end{bmatrix}, \tag{2}$$

and the potential energy function

$$\mathcal{U}(q_1, q_2) = m_3[\cos(q_1) - 1] \tag{3}$$

being $a_1 = I_1 + I_2$, $a_2 = I_2$, $a_3 = I_2$, and to simplify notation, we have defined

$$m_3 \triangleq g(m_1 l_{c_1} + m_2 l_1) \tag{4}$$

and in turn, we have considered $(I_1 + I_2) >> (m_1 l_{c_1}^2 + m_2 l_1^2)$. From Figure 1, θ_1 and θ_2 are the joint positions of the pendulum and the wheel, respectively, and u is the control torque input acting between wheel and pendulum. Following the same assumption made in Ortega et al. (2002), it has been assumed both mechanism joints without friction. The meaning of the remaining parameters is listed in Table 1.

Table 1. Parameters

Description	*Notation*	*Units*
Length of the pendulum	l_1	m
Distance at the center of mass of the pendulum	l_{c1}	m
Mass of the pendulum	m_1	kg
Mass of the disk	m_2	kg
Moment of inertia of the pendulum	I_1	kg.m^2
Moment of inertia of the disk	I_2	kg.m^2
Gravity acceleration	g	m/s^2

The momentum $\boldsymbol{p}$ is defined as (Nijmeijer & Van der Schaft (1990)):

$$\boldsymbol{p} = M\dot{\boldsymbol{q}} \tag{5}$$

where $\dot{\boldsymbol{q}}$ is the vector of generalized velocities. The dynamic model of the torque–driven inertia wheel pendulum without viscous friction, can be written as (Ortega et al. (2002)):

$$\frac{d}{dt}\begin{bmatrix} \boldsymbol{q} \\ \boldsymbol{p} \end{bmatrix} = \begin{bmatrix} 0_{2\times 2} & I_{2\times 2} \\ -I_{2\times 2} & 0_{2\times 2} \end{bmatrix} \begin{bmatrix} \nabla_{\boldsymbol{q}} H(\boldsymbol{q}, \boldsymbol{p}) \\ \nabla_{\boldsymbol{p}} H(\boldsymbol{q}, \boldsymbol{p}) \end{bmatrix} + \begin{bmatrix} \mathbf{0}_2 \\ G \end{bmatrix} u \tag{6}$$

where

$$G = \begin{bmatrix} 0 \\ 1 \end{bmatrix}, \tag{7}$$

and u is the torque control input, which is used to provide the motion θ_2, and this in turn indirectly produces the motion θ_1. Considering (1), (2) and (3) into (6) yields

$$\frac{d}{dt}\begin{bmatrix} q_1 \\ q_2 \\ p_1 \\ p_2 \end{bmatrix} = \begin{bmatrix} \dfrac{[a_3 p_1 - a_2 p_2]}{\det[M]} \\ \dfrac{[-a_2 p_1 + a_1 p_2]}{\det[M]} \\ m_3 \sin(q_1) \\ u \end{bmatrix} \tag{8}$$

We can now formulate the control problem under actuator torque constraints addressed in this work. Consider the inertia wheel pendulum model (8). Assume the ideal torque actuator is able to supply a known maximum torque u^{max} such that

$$|u(t)| \leq u^{max}. \tag{9}$$

We also assume that the maximum torque satisfies the following condition:

$$u^{max} > m_3 \tag{10}$$

where m_3 is defined in (4). Formally, the control objective is

$$\lim_{t\to\infty} \begin{bmatrix} q_1(t) \\ \dot{q}_2(t) \end{bmatrix} = \begin{bmatrix} 0 \\ r \end{bmatrix}, \text{ and } |u(t)| \leq u^{max}, \tag{11}$$

where $r \geq 0$ is the user selected desired speed of the wheel. However, the value of r is not arbitrary but it is limited by the domain of attraction which $u(t)$ achieves the control objective (11). The computing of this domain of attraction is beyond of the present paper.

3. CONTROLLER DESIGN

3.1 Previous work

Based on an alternative energy shaping and damping injection approach, the following control law was proposed in Sandoval et al. (2020):

$$\begin{aligned} u = {} & k_p k_1 [q_{a_2} - \gamma_2 q_{a_1}] - k_v k_2 [-p_{a_1} + p_{a_2}] \\ & + \gamma_1 \sin\left(\frac{q_{a_1}}{a_1} + \bar{q}_{d_1}\right), \end{aligned} \tag{12}$$

where the following coordinates transformation has been entered:

$$\begin{bmatrix} q_{a_1} \\ q_{a_2} \end{bmatrix} = \begin{bmatrix} a_1 q_1 \\ a_2[q_2 - rt] \end{bmatrix}, \text{ and } \begin{bmatrix} p_{a_1} \\ p_{a_2} \end{bmatrix} = \begin{bmatrix} d_1 \dot{q}_{a_1} + d_2 \dot{q}_{a_2} \\ d_2 \dot{q}_{a_1} + d_3 \dot{q}_{a_2} \end{bmatrix}, \tag{13}$$

being $\gamma_2 = \frac{(d_1 - d_2)}{(d_3 - d_2)}$, while k_p and k_v are arbitrary strictly positive constants, and the d_i elements are chosen to hold the inequalities:

$$d_1 > d_3, \text{ and } d_2 > d_3, \tag{14}$$

such that $d_1 d_3 - d_2^2 > 0$. Finally, the k_1, k_2, γ_1 strictly positive constants are given by:

$$\begin{aligned} k_1 &= \frac{1}{\det[M_a]}\left[\left[-\frac{a_2}{a_1}d_3 + \frac{a_3}{a_2}d_2\right] + \gamma_2\left[\frac{a_2}{a_1}d_2 - \frac{a_3}{a_2}d_1\right]\right], \\ k_2 &= \frac{a_1 a_2}{\det[M]}, \\ \gamma_1 &= -\frac{m_3}{[d_3 - d_2]}\left[-\frac{a_2}{a_1}d_3 + \frac{a_3}{a_2}d_2\right]. \end{aligned}$$

As pointed out in Sandoval et al. (2020), the control law (12) is the sum of two terms

$$u = u_{es} + u_{di}$$

where

$$u_{es} = k_p k_1 [q_{a_2} - \gamma_2 q_{a_1}] + \gamma_1 \sin\left(\frac{q_{a_1}}{a_1} + \bar{q}_{d_1}\right), \tag{15}$$

$$u_{di} = -k_v k_2 [-p_{a_1} + p_{a_2}]. \tag{16}$$

The term u_{es} is designed to achieve the energy shaping and u_{di} injects the damping to the closed–loop system. Hence, the control law (12) can be rewritten as

$$\begin{aligned} u = &\underbrace{k_p k_1 [q_{a_2} - \gamma_2 q_{a_1}] + \gamma_1 \sin\left(\frac{q_{a_1}}{a_1} + \bar{q}_{d_1}\right)}_{u_{es}} \\ &\underbrace{-k_v k_2 [-p_{a_1} + p_{a_2}]}_{u_{di}}. \end{aligned} \tag{17}$$

Remark 1: From the definition (13), we obtain the velocity vector $\dot{\boldsymbol{q}}_a = [\dot{q}_{a_1} \;\; \dot{q}_{a_2}]^T = [a_1 \dot{q}_1 \;\; a_2[\dot{q}_2 - r]]^T$, and substituting this identity into (12), the control law may be rewritten in a compact way:

$$\begin{aligned} u = &k_p k_1 [q_{a_2} - \gamma_2 q_{a_1}] - k_v k_2 [[-d_1 + d_2]\dot{q}_{a_1} + [d_2 + d_3]\dot{q}_{a_2}] \\ &+ \gamma_1 \sin\left(\frac{q_{a_1}}{a_1} + \bar{q}_{d_1}\right). \end{aligned} \tag{18}$$

Notice that (18) has a PD-like structure plus a nonlinear term given by the third addend.

$\diamond\diamond$

Closed–loop system A detailed stability analysis —in Lagrangian formulation— of the equilibria of the closed–loop system formed by the control law (12) and the Hamiltonian system (8), shown at the next page by (19), was presented in Sandoval et al. (2020). It is easy to note that the equilibrium set is

$$E = \begin{bmatrix} q_{a_1 *} \\ q_{a_2 *} \\ p_{a_1 *} \\ p_{a_2 *} \end{bmatrix} = \begin{bmatrix} a_1[\delta\pi - \bar{q}_{d_1}] \\ \gamma_2 a_1 [\delta\pi - \bar{q}_{d_1}] \\ 0 \\ 0 \end{bmatrix} \tag{20}$$

In acccordance with (11), we consider the origin as the equilibrium of interest, that is, $[q_{a_1}^* \;\; q_{a_2}^*]^T = [0 \;\; 0]^T$ which is achieved with $\bar{q}_{d_1} = \delta\pi$. By simplicity, we have considered $\delta = 0$ such that $\bar{q}_{d_1} = 0$.

3.2 Proposed controller

By bearing in mind, the actuator torque constraints control problem, addressed in this work, we can modify the control law (12) in order to have bounded all its terms. To this end, following similar steps to those in Sandoval et al. (2020), we can propose the new energy shaping term

$$u_{es} = k_p k_1 \tanh(q_{a_2} - \gamma_2 q_{a_1}) + \gamma_1 \sin\left(\frac{q_{a_1}}{a_1} + \bar{q}_{d_1}\right).$$

This new u_{es} is the result of proposing the following desired potential energy function:

$$\begin{aligned} \mathcal{U}_a(q_{a_1}, q_{a_2}) = &\frac{a_1 m_3 \det[M_a]}{[d_3 - d_2]}\left[\cos\left(\frac{q_{a_1}}{a_1} + \bar{q}_{d_1}\right) - 1\right] \\ &+ \frac{1}{2}k_p \ln(\cosh(q_{a_2} + \gamma_2 q_{a_1})), \end{aligned} \tag{21}$$

where the matrix M_a is composed by

$$M_a = \begin{bmatrix} d_1 & d_2 \\ d_2 & d_3 \end{bmatrix}. \tag{22}$$

Besides, because we require bounded control action, we propose the damping injection term u_{di} as:

$$u_{di} = -k_v k_2 \tanh[-p_{a_1} + p_{a_2}] \tag{23}$$

which still preserve the passivity property of the new closed–loop system (24), shown at the top of the next page. Therefore, we propose the following control law:

$$\begin{aligned} u = &\underbrace{k_p k_1 \tanh[q_{a_2} - \gamma_2 q_{a_1}] + \gamma_1 \sin\left(\frac{q_{a_1}}{a_1} + \bar{q}_{d_1}\right)}_{u_{es}} \\ &\underbrace{-k_v k_2 \tanh[-p_{a_1} + p_{a_2}]}_{u_{di}}. \end{aligned} \tag{25}$$

The positive constants $k_p k_1$ and $k_v k_2$ must be chosen sufficiently small. More specifically, they must satisfy

$$u^{max} - \gamma_1 > k_p k_1 - k_v k_2.$$

It is worth noticing that all terms in (25) are bounded; furthermore, the control law is bounded by

$$\begin{aligned} |u| &\leq \gamma_1 + k_p k_1 - k_v k_2 \\ &\leq u^{max}. \end{aligned} \tag{26}$$

4. STABILITY ANALYSIS

A feature of the alternative energy shaping and damping injection approach is that the desired energy function used to design the proposed control law (25) qualifies as a Lyapunov function candidate $V(\boldsymbol{q}_a, \boldsymbol{p}_a)$. Hence, to carry out the stability analysis we propose

$$\begin{aligned} V(\boldsymbol{q}_a, \boldsymbol{p}_a) = &\frac{1}{2\det[M_a]}[d_3 p_{a_1}^2 - 2d_2 p_{a_1} p_{a_2} + d_1 p_{a_2}^2] \\ &\frac{a_1 m_3 \det[M_a]}{[d_3 - d_2]}\left[\cos\left(\frac{q_{a_1}}{a_1} + \bar{q}_{d_1}\right) - 1\right] \\ &+ \frac{1}{2}k_p \ln(\cosh(q_{a_2} + \gamma_2 q_{a_1})), \end{aligned} \tag{27}$$

where $\det[M_a] = d_1 d_3 - d_2^2$.

The closed-loop system is obtained combining the control law (25) and the open–loop system (8), which yields (24),

$$\frac{d}{dt}\begin{bmatrix} q_{a_1} \\ q_{a_2} \\ p_{a_1} \\ p_{a_2} \end{bmatrix} = \begin{bmatrix} \frac{1}{\det[M_a]}[d_3 p_{a_1} - d_2 p_{a_2}] \\ \frac{1}{\det[M_a]}[-d_2 p_{a_1} + d_1 p_{a_2}] \\ \frac{m_3 \det[M_a]}{[d_3 - d_2]} \sin\left(\frac{q_{a_1}}{a_1} + \bar{q}_{d_1}\right) + \gamma_2 k_p (q_{a_2} - \gamma_2 q_{a_1}) - \frac{k_v [d_1 - d_2]}{\det[M]}(-p_{a_1} + p_{a_2}) \\ -k_p \tanh[q_{a_2} - \gamma_2 q_{a_1}] - \frac{k_v [d_3 - d_2]}{\det[M]}(-p_{a_1} + p_{a_2}) \end{bmatrix} \tag{19}$$

$$\frac{d}{dt}\begin{bmatrix} q_{a_1} \\ q_{a_2} \\ p_{a_1} \\ p_{a_2} \end{bmatrix} = \begin{bmatrix} \frac{1}{\det[M_a]}[d_3 p_{a_1} - d_2 p_{a_2}] \\ \frac{1}{\det[M_a]}[-d_2 p_{a_1} + d_1 p_{a_2}] \\ \frac{m_3 \det[M_a]}{[d_3 - d_2]} \sin\left(\frac{q_{a_1}}{a_1} + \bar{q}_{d_1}\right) + \gamma_2 k_p \tanh(q_{a_2} - \gamma_2 q_{a_1}) - \frac{k_v [d_1 - d_2]}{\det[M]} \tanh(-p_{a_1} + p_{a_2}) \\ -k_p \tanh[q_{a_2} - \gamma_2 q_{a_1}] - \frac{k_v [d_3 - d_2]}{\det[M]} \tanh(-p_{a_1} + p_{a_2}) \end{bmatrix} \tag{24}$$

shown at the top of this page. Notice that the equilibrium set is

$$\mathcal{E} = \begin{bmatrix} q_{a_1 *} \\ q_{a_2 *} \\ p_{a_1 *} \\ p_{a_2 *} \end{bmatrix} = \begin{bmatrix} a_1[\delta\pi - \bar{q}_{d_1}] \\ \gamma_2 a_1 [\delta\pi - \bar{q}_{d_1}] \\ 0 \\ 0 \end{bmatrix}. \tag{28}$$

In acccordance with (11), we consider the origin as the equilibrium of interest, that is, $[q_{a_1}^* \;\; q_{a_2}^*]^T = [0 \;\; 0]^T$ which is achieved with $\bar{q}_{d_1} = \delta\pi$. By simplicity, we have considered $\delta = 0$ such that $\bar{q}_{d_1} = 0$. We have ommited, due to paper length reasons, the proof that verify the local positive definiteness of $V(\boldsymbol{q}_a, \boldsymbol{p}_a)$ for n even.

The time derivate of function (27) along the trajectories of the closed-loop equation (24) becomes

$$\dot{V}(\boldsymbol{q}_a, \boldsymbol{p}_a) = -k_v k_2 [-p_{a_1} + p_{a_2}] \tanh(-p_{a_1} + p_{a_2}) \tag{29}$$

which is a negative semidefinite function, because by design $k_v k_2 > 0$.

Because the closed-loop equation (24) is autonomous, we can use the Barbashin–Krasovskii's theorem to prove that origin in the set $\mathcal{E}$ is asymptotically stable (Khalil (2002)). Thus, it is convenient to define $\mathcal{B} \subset \mathbb{R}^4$ as

$$\mathcal{B} = \left\{ \begin{bmatrix} \boldsymbol{q}_a \\ \boldsymbol{p}_a \end{bmatrix} \in \mathbb{R}^4 : q_{a_1} \in \left(-\frac{a_1\pi}{2}, \frac{a_1\pi}{2}\right), \right.$$
$$\left. q_{a_2} \in (-\gamma_2 a_1 \pi, \gamma_2 a_1 \pi) \right\} \tag{30}$$

So, the unique equilibrium in $\mathcal{B}$ is the origin of the state space. Next, we introduce a procedure inspired in the stability analysis developed by Gandarilla et al. (2019) to ensure asymptotic stability of the origin, which is based on the Barbashin–Krasovskii's theorem. Toward this end, we provide the following results. Notice that $V(\boldsymbol{q}_a, \boldsymbol{p}_a)$ is a locally positive definite function and its time derivative along the trajectories of (24) is a negative semi-definite function, given by (29). Continuing with the steps required by the Barbashin–Krasovskii's theorem, we define the S set as:

$$S = \left\{ \begin{bmatrix} \boldsymbol{q}_a \\ \boldsymbol{p}_a \end{bmatrix} \in \mathcal{B} : -p_{a_1} + p_{a_2} = 0 \right\}. \tag{31}$$

The next step is to prove that no solution can stay identically in S, other than the trivial solution, that is, $[q_{a_1} \;\; q_{a_2} \;\; p_{a_1} \;\; p_{a_2}]^T = [0 \;\; 0 \;\; 0 \;\; 0]^T$. This is equivalent to demonstrate than the largest invariant set into S is this trivial solution. Towards this end, we recall that an invariant set inside of the S set must to accomplish (Haddad & Chellaboina (2008), pp. 147-148):

$$\frac{d}{dt}[-p_{a_1} + p_{a_2}] = 0,$$
$$-\dot{p}_{a_1} + \dot{p}_{a_2} = 0. \tag{32}$$

Moreover, in accordance with the definiton (13), the equation inside (31) may be rewritten as

$$\dot{q}_{a_2} - \gamma_2 \dot{q}_{a_1} = 0.$$

Then, by integrating the above equation, it yields

$$\int_0^t [\dot{q}_{a_2}(\sigma) - \gamma_2 \dot{q}_{a_1}(\sigma)] d\sigma = 0,$$
$$[q_{a_2}(t) - \gamma_2 q_{a_1}(t)] - \kappa = 0,$$
$$z(q_{a_1}, q_{a_2}) - \kappa = 0, \tag{33}$$

where $z(q_{a_1}, q_{a_2}) = q_{a_2}(t) - \gamma_2 q_{a_1}(t)$, and κ is some specific constant to find. Thus, an invariant set inside of the S set must also meet:

$$z(q_{a_1}, q_{a_2}) = \kappa. \tag{34}$$

In order to simplify our analysis, considering (31) and (34) into (24), we reduce the closed-loop system (24) as follows:

$$\frac{d}{dt}\begin{bmatrix} q_{a_1} \\ q_{a_2} \\ p_{a_1} \\ p_{a_2} \end{bmatrix} = \begin{bmatrix} \frac{[d_3 - d_2] p_{a_2}}{\det[M_a]} \\ \frac{[d_1 - d_2] p_{a_2}}{\det[M_a]} \\ \frac{m_3 \det[M_a]}{[d_3 - d_2]} \sin\left(\frac{q_{a_1}}{a_1}\right) - \gamma_2 k_p \tanh(\kappa) \\ -k_p \tanh(\kappa) \end{bmatrix} \tag{35}$$

From (35), notice that $\dot{p}_{a_2} = -k_p \tanh(\kappa)$, thereby integrating respect to the time is possible to arrive at the next result:

$$p_{a_2} = -k_p \tanh(\kappa) t + C_1, \tag{36}$$

where C_1 is an arbitrary constant. As previously demonstrated the origin is a stable equilibrium point, then the trajectories $[q_{a_1}(t) \;\; q_{a_2}(t) \;\; p_{a_1}(t) \;\; p_{a_2}(t)]^T$ of the closed-loop system (24) starting sufficiently close of the origin, trajectories can be guaranteed to stay within any specified ball centered at the origin, thus inside this region (specified ball centered at the origin) $p_{a_2}(t)$ is bounded (it cannot grow indefinitely with respect to the time), then $\kappa = 0$ and this one implies $p_{a_2} = C_1$ and $\dot{p}_{a_2} = 0$ from (36) and (35), respectively; from (35) it means that variable p_{a_2} remains constant. Considering the above result into (35) it gets

$$\frac{m_3 \det[M_a]}{(d_3 - d_2)} \sin\left(\frac{q_{a_1}}{a_1}\right) = 0 \qquad (37)$$

whose unique solution is $q_{a_1} = 0$ for $q_{a_1} \in \left(-\frac{a_1\pi}{2}, \frac{a_1\pi}{2}\right)$. Replacing $q_{a_1} = 0$ and $\kappa = 0$ into (34) result $q_{a_2} = 0$, which implies $\dot{q}_{a_1} = \dot{q}_{a_2} = 0$, and its in turn it gets $p_{a_1} = p_{a_2} = 0$. It means that the equilibrium point in the origin $[q_{a_1} \;\; q_{a_2} \;\; p_{a_1} \;\; p_{a_2}]^T = [0 \;\; 0 \;\; 0 \;\; 0]^T$ is the largest invariant set inside the S set. Then, by theorem of Barbashin–Krasovskii we conclude that this equilibrium point is locally asymptotically stable and the control objective (11) is ensured in a local sense.

So we have proven the following:

Proposition. For an enough small desired wheel speed r, the inertia wheel pendulum (8) in closed-loop with the bounded control law (25) has an isolated locally asymptotically stable equilibria. Furthermore, the applied torque is bounded by

$$|u| \le u^{max}.$$

$\diamond\diamond\diamond$

5. SIMULATION RESULTS

In this section we present the simulation results obtained on an inertia wheel pendulum model by using the parameters given in Sandoval et al. (2020). These correspond to $m_3 = 10$, $I_1 = 0.1$, $I_2 = 0.2$. We suppose the maximum torque that can supply the actuator is $u^{max} = 35$ Nm. The remaining parameters were selected as $d_1 = 5$, $d_2 = 2$ and $d_3 = 1$, which ensure positivity of the M_a matrix. The gains were chosen as $k_p = 2.0$ and $k_v = 2.0$, so that, we calculate the constants: $\gamma_1 = 0.05$, $k_p k_1 = 39$ and $k_v k_2 = 6$. Substituting these values in the control law (25), we have

$$|u| < \gamma_1 + k_p k_1 - k_v k_2 = 33.05 \text{ Nm} < u^{max}, \qquad (38)$$

The initial configuration considered the pendulum position on the horizontal: $[q_1(0) \;\; q_2(0) \;\; p_1(0) \;\; p_2(0)]^T = [85.9^{\circ} \;\; 0 \;\; 1.0 \;\; 0]^T$, and a desired constant speed $r = 10$ [rad/s]. MATLAB software was utilized for numeric simulations with ODE23 solver, which is based on an explicit Runge-Kutta formula, the Dormand-Prince pair, where we have used a relative error tolerance of 1×10^{-3}.

The plots depicted in Figures 2 and 3 show that the q_1 joint position and the wheel speed $\dot{q}_2$ vanish towards the desired values, such that the objective control (11) is achieved. Notice that the bounded torque (25) clearly evolves inside the prescribed limit –depicted with red dotted lines– given in (38) with a maximum torque of 14.08 Nm, while the non-bounded torque (12) achieves values greater than $u^{max} = 35$ Nm, specifically in the initial time.

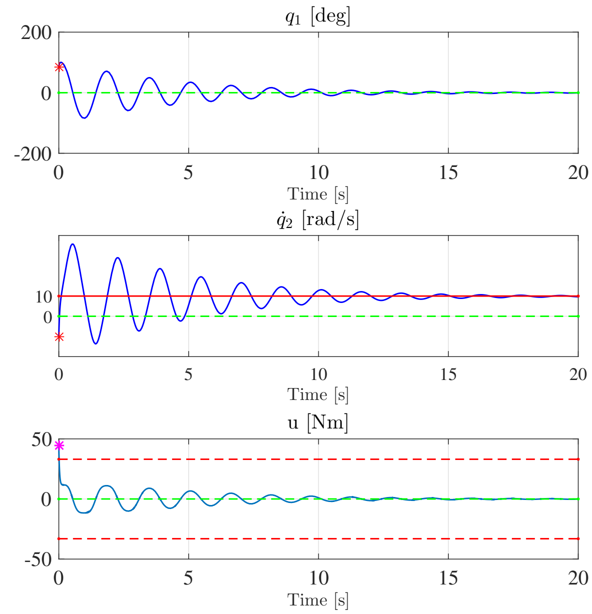

Fig. 2. Time evolution of the $q_1(t)$ joint position, the $\dot{q}_2$ speed wheel, and the non-bounded torque control input given by (12).

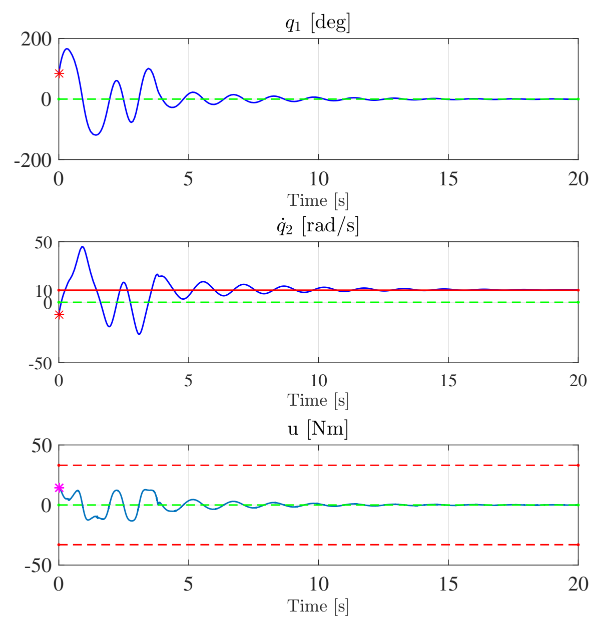

Fig. 3. Time evolution of the $q_1(t)$ joint position, the $\dot{q}_2$ speed wheel, and the bounded torque control input given by (25).

6. CONCLUSIONS

We have proposed a speed control scheme with bounded torque for the inertia wheel pendulum. The proposed controller was designed following an alternative energy shaping and damping injection approach, but now taking care in the actuator torque restriction. Conditions on the controller gains are provided to guarantee that the control action remains within the prescribed limit.

ACKNOWLEDGEMENTS

The first author thanks Isaac Gandarilla, from Instituto Tecnológico de La Laguna, for his valuable support in the asymptotic stability analysis.

REFERENCES

Bloch, A. M., Leonard, N. & Marsden, J. (2000). Controlled Lagrangian and the stabilization of mechanical systems. *IEEE Transactions on Automatic Control*, 45(12), 2253–2270.

Delgado, S. & Kotyczka, P. (2016). Energy shaping for position and speed control of a wheeled inverted pendulum in reduced space. *Automatica*, 74, 222–229.

Gandarilla, I., Santibáñez, V. & Sandoval, J. (2019). Control of a self-balancing robot with two degrees of freedom via IDA-PBC. *ISA Transactions*, 88, 102–112.

Haddad, W.,& Chellaboina, V. (2008). *Nonlinear dynamical systems and control*. Princeton, NJ, USA: Princeton University Press.

Khalil, H. K. (2002). *Nonlinear systems* (3rd ed.), Upper Saddle River, NJ, USA: Prentice-Hall.

Nijmeijer H. and Van der Schaft A. (1990), *Nonlinear dynamical control systems*, Springer-Verlag New York, USA.

Ortega, R., Spong, M. W., Gómez-Estern, F., & Blankenstein, G. (2002). Stabilization of a class of underactuated mechanical systems via interconnection and damping assignment. *IEEE Transactions on Automatic Control*, 47(8), 1213–1233.

Romero, J., Ortega, R. & Donaire, A. (2016), Energy shaping of mechanical systems via PID control and extension to constant speed tracking, *IEEE Transactions on Automatic Control*, vol. 61, pp. 3551–3556.

Sandoval, J., Kelly, R., & Santibáñez, V. (2020). A speed regulator for a torque–driven inertia wheel pendulum, *Preprints of the 21st IFAC World Congress (Virtual)* (pp. 6371–6376), Berlin, Germany, July 12-17.

Santibáñez, V., Kelly, R. & Sandoval, J. (2005) Control of the inertia wheel pendulum by bounded torques. *In 44th IEEE Conference on Decision and Control and 2005 European Control Conference, CDC-ECC'05* (pp. 8266–8270), Seville, Spain.

